

See discussions, stats, and author profiles for this publication at: <https://www.researchgate.net/publication/258239280>

Chemical Engineering Journal 1

DATASET · NOVEMBER 2013

READS

54

4 AUTHORS, INCLUDING:



[Subrahmanyam Challapalli](#)

Indian Institute of Technology Hyderabad

111 PUBLICATIONS **1,055** CITATIONS

SEE PROFILE



[Ramasamy Karvembu](#)

National Institute of Technology Tiruchirap...

132 PUBLICATIONS **1,493** CITATIONS

SEE PROFILE



[Karuppiah Jaya](#)

Jeju National University

28 PUBLICATIONS **118** CITATIONS

SEE PROFILE



Catalytic nonthermal plasma reactor for the abatement of low concentrations of isopropanol

J. Karupiah^a, L. Sivachandiran^b, R. Karvembu^a, Ch. Subrahmanyam^{b,*}

^a Department of Chemistry, National Institute of Technology Trichy, Tiruchirappalli 620015, India

^b Department of Chemistry, Indian Institute of Technology Hyderabad, Yeddumailaram, Hyderabad 502205, India

ARTICLE INFO

Article history:

Received 5 July 2010

Received in revised form

14 September 2010

Accepted 15 September 2010

Keywords:

Dielectric barrier discharge

Isopropanol

Specific input energy

Sintered metal fibres

Ozone

ABSTRACT

Oxidative decomposition of a model volatile organic compound (isopropanol, IP) has been carried out in a catalytic dielectric barrier discharge (DBD) reactor, where modified sintered metal fiber (SMF) filter was used as the inner electrode. The SMF was modified with Mn and Co oxides by impregnation, followed by calcination and the performance of the DBD reactor was tested for the oxidation of IP in the specific input energy range 160–720 J/l by varying the high voltage and frequency. It has been observed that SMF modification by MnO_x and CoO_x not only improved the conversion of isopropanol, but also increased the selectivity towards total oxidation. MnO_x modification showed better performance than CoO_x, which may be attributed to the formation of atomic oxygen by *in situ* decomposition of ozone. It has been demonstrated that with MnO_x/SMF it is possible to completely oxidize 100 ppm of isopropanol at SIE < 200 J/l.

© 2010 Elsevier B.V. All rights reserved.

1. Introduction

Isopropanol (IP) is widely used as a solvent and cleaning fluid, especially for dissolving lipophilic contaminants such as oil [1]. The uses of IP include cleaning electronic devices such as contact pins, disk heads, the lenses of lasers in optical disc drives. It is also used to clean LCD and computer monitor screens [1,2]. It is also effective at removing residual glue from some sticky labels. It can also be used to remove stains from most fabrics, wood, cotton, etc. Isopropyl alcohol vapor is denser than air and is highly flammable. It should be kept away from heat and flame [2,3]. On mixing with air or other oxidizers, IP can explode through deflagration. Its odor threshold has been estimated as 22 ppm and recommended exposure limit in the work place is 400 ppm. Exposure to higher concentration of IP may cause health problems like irritation of eyes, drowsiness, and dizziness. Isopropyl alcohol is oxidized by the liver into acetone by alcohol dehydrogenase. Symptoms of isopropyl alcohol poisoning include flushing, headache, dizziness, CNS depression, nausea, vomiting, anesthesia, and coma and hence its abatement if warranted. Excess of isopropanol will be separated from water and other by-products by distillation. Isopropyl alcohol and water form an azeotrope and simple distillation gives a material which is 87.9% by weight isopropyl alcohol and 12.1% by weight

water. The usual practice to remove IP from industrial effluent is by absorption into water by using wet scrubbers followed by distillation or pervaporation. Thermal oxidation of alcohols needs a high temperature in the range 600–700 °C, whereas, catalytic oxidation will be carried out in the temperature range 250–350 °C [4,5].

Even though these techniques are promising, at low concentrations (<1000 ppm) these techniques are energetically not favorable as abatement of dilute VOCs under low concentrations needs continuous supply of heat energy.

In this context, non-thermal plasma (NTP) generated at atmospheric pressure is an alternate method of choice, mainly due to ease of operation under ambient conditions [5–18]. At dilute pollutant concentrations, typically less than 1000 ppm, NTP treatment requires less energy than incineration or thermal-plasma treatment. In many case studies it has been reported to be economical than raising the temperature of the entire gas stream to temperatures needed for catalytic decomposition (200–500 °C). In NTP, the electrical energy is primarily utilized for the production of energetic electrons, leaving the background gas nearly at room temperature [15–25]. In addition, when operated in air, NTP produces potentially active species like N₂⁺ (A³Σ_u⁺), N₂⁺ (B³Π_u⁺), O₂⁺ (a¹Δ_g), O(¹D), O(³P), and N(⁴S) in addition to ozone. The NTP technique was tested for the destruction of IP with an input energy of 400 and 700 J/l, respectively during the destruction of 135 and 400 ppm of IP [13]. However, formation of a stable secondary product acetone was observed, whose destruction demands still higher energy (~1100 J/l), which is not economical [4]. Hence, decreasing the

* Corresponding author. Fax: +91 40 2301 6032.

E-mail addresses: csubbu@iith.ac.in, challa168@hotmail.com (Ch. Subrahmanyam).

input energy and improving the reactor performance towards total oxidation of IP is warranted.

Recently we reported a novel DBD reactor configuration with a metallic catalyst made of sintered metal fibres (SMF) also served as the inner electrode [26,27]. Destruction of various VOCs was tested over modified SMF electrodes and typical results indicate that with a suitable modification of SMF with various transition metal oxides, complete oxidation of VOCs was achieved at low consumption of energy [26–28]. The designed reactor was earlier tested for the destruction of IPA at a fixed concentration of 250 ppm over MnO_x/SMF . However, there is a need to study the performance of the NTP reactor as a function of IP concentration in order to exploit the potentials of NTP technique, especially for lower concentrations. During the present study, performance of the DBD reactor has been tested for the IPA total oxidation [28]. Influence of various parameters like the selection of the catalyst, applied voltage, frequency, concentration of IP and the formation of ozone on the performance of plasma reactor will be discussed.

2. Experimental

2.1. Materials and methods

Sintered metal fiber filters (SMF, Southwest Screens & Filters SA, Belgium) made of stainless steel consisting of thin uniform metal fibers of diameter 30 μm , wetness capacity of ~30 wt% and porosity of ~80 wt% were used in the present study. For the preparation of 3 wt% MnO_x and CoO_x , the SMF was oxidized at 873 K for 3 h, followed by impregnation with Co and Mn nitrate aqueous solutions of desired concentration. Drying at room temperature followed by calcination in air at 773 K for 5 h resulted in catalytic electrodes of metal oxide supported on SMF. The CoO_x and MnO_x/SMF contained 3 wt% of the metal oxide. XPS analysis confirmed the formation of metal oxides on SMF [26]. Finally, SMF filters were subjected to an electrical hot press to shape them into cylindrical form giving the desired discharge gap.

2.2. Plasma reactor

A detailed description of the DBD reactor is reported elsewhere [26]. Briefly, the dielectric discharge was generated in a cylindrical quartz tube with an inner diameter of 18.5 mm. A silver paste painted on the outer surface of the quartz tube acted as the outer electrode, where a modified SMF acts as the inner electrode. The discharge length was 10 cm and discharge gap was fixed at 3.5 mm during the destruction of IP. The specific input energy (SIE) in the range 160–725 J/l was applied by varying the AC high voltage (12.5–22.5 kV) and frequency (200–275 Hz). Conversion of VOC at each voltage was measured after 30 min. A voltage (V)–charge (Q) Lissajous method was used to determine the discharge power (W) in the plasma reactor, where the charge Q (i.e. time integrated current) was recorded by measuring the voltage across the capacitor of 220 nF connected to the ground electrode. The voltage was measured with a high voltage probe (Luke 80 K–40 HV). The signals of V and Q were recorded with a digital oscilloscope (Tektronix, TDS 3054) and plotted to get a typical V–Q Lissajous diagram.

2.3. Experimental procedure

The experimental set-up consisted of a motor driven syringe pump for the introduction of IP, which was mixed with 500 ml/min (STP) air and was fed into the plasma reactor with a Teflon tube. IP concentration at the outlet of the reactor was measured with a gas chromatograph (Varian 450) equipped with a flame ionization detector. The formation of CO_2 and CO was simultaneously monitored with an infrared gas analyzer (Analyzer instruments

company, India), whereas ozone formed in the plasma reactor was measured with a UV absorption ozone monitor (API-450 NEMA). As the volume change due to chemical reactions is negligible, selectivity to CO_2 and CO_x was defined as follows:

$$S_{\text{CO}}(\%) = \frac{[\text{CO}]}{3([\text{VOC}]_0 - [\text{VOC}])} \times 100$$

$$S_{\text{CO}_2}(\%) = \frac{[\text{CO}_2]}{3([\text{VOC}]_0 - [\text{VOC}])} \times 100$$

$$S_{\text{CO}_x} = S_{\text{CO}} + S_{\text{CO}_2}$$

3. Results and discussion

3.1. Performance of DBD reactor during the decomposition of IP

NTP technique is expected to be advantageous especially for VOC concentration ≤ 1000 ppm as it is difficult to maintain adiabatic conditions under such dilute concentrations. During the present study, concentration of IP has been changed between 100 and 1000 ppm in order to understand the influence of VOC concentration on the performance of the reactor. Fig. 1 presents the activity of various catalytic electrodes during the conversion of 1000 ppm of IP in the applied voltage range 12.5–22.5 kV that corresponds to the SIE of 160–295 J/l, respectively. As seen from Fig. 1, conversion of IP

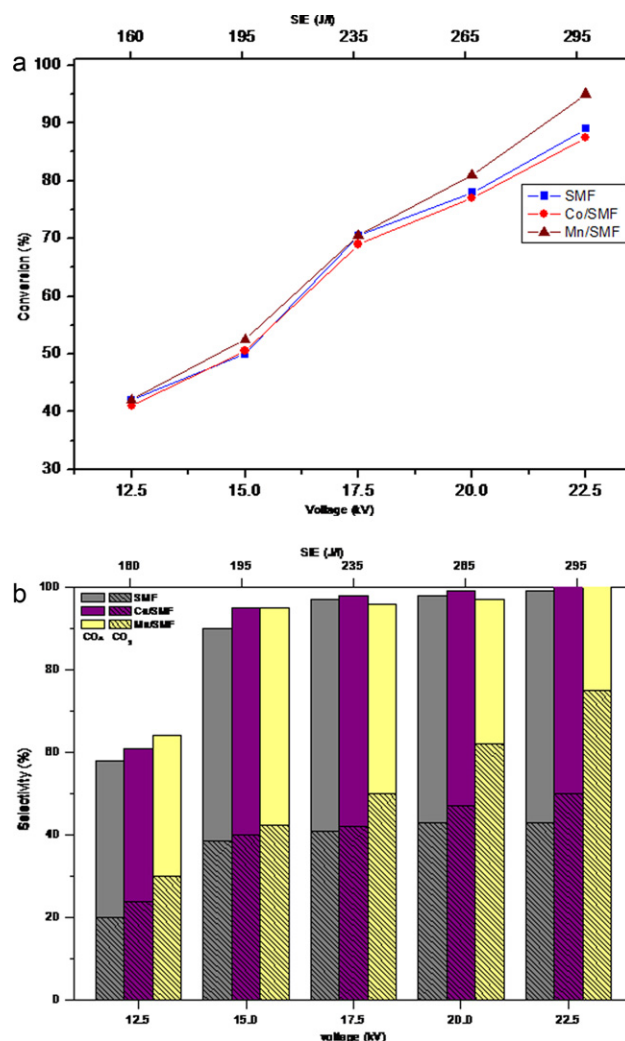


Fig. 1. (a) Influence of SMF modification and SIE on the conversion of IP (SIE 160–295 J/l and 1000 ppm of IP). (b) Influence of SMF modification and SIE on selectivity to CO_x and CO_2 (SIE 160–295 J/l and 1000 ppm of IP).

increases with increasing SIE over all the electrodes from ~40% at 165 J/l to more than 90% at 295 J/l. Also, as seen from Fig. 1 SMF modification with transition metal oxides has not shown any significant influence. This may be due to the quick deactivation of the catalyst by polymeric products formed in the reaction, which is in agreement with the earlier observation during the abatement of IP [28].

During the decomposition of any VOC, the desired products are CO_2 and H_2O , i.e. total oxidation. However, as the NTP abatement of VOCs may lead to undesired and sometimes toxic by-products like CO, in general, the selectivity to CO_2 is not 100%. During the present study as no other hydrocarbon except IP was detected at the outlet, CO_x selectivity also represents the carbon balance. Figure 1b presents the CO_x ($\text{CO} + \text{CO}_2$) selectivity and also the carbon balance. The selectivity to CO_x was close to 60% with all catalysts and was never 100%. But with increasing SIE, the CO_x selectivity also increases and reached 100% at 295 J/l. Hence, for 1000 ppm of IP in the SIE range of the present study, the SMF catalytic electrodes showed poor carbon balance and considerable amount of carbon was deposited on the walls of the reactors. However, as seen from Fig. 1b, SMF modification with CoO_x and MnO_x resulted higher CO_x selectivity. Fig. 1b also presents the CO_2 selectivity. As seen from Fig. 1b, the selectivity to CO_2 also followed a similar trend to that of CO, where SMF electrode showed ~20% selectivity at 160 J/l, whereas, CoO_x and MnO_x modified SMF electrodes showed 30% selectivity. With increasing SIE, CoO_x and MnO_x modified electrodes showed higher selectivity, whereas, SMF showed a maximum of 40% even at 295 J/l.

During the destruction of 1000 ppm of IP, conversion and CO_2 selectivity were not 100%, which may be due to high concentration of IP (Fig. 1a and b). In order to understand the influence of inlet concentration, IP concentration has been varied between 1000 and 100 ppm. Fig. 2 presents the performance of the catalytic DBD reactor for destruction of 500 ppm of IP. As seen from Fig. 2a, decreasing IP concentration from 1000 ppm to 500 ppm did not show any significant change in conversion. However, as seen from Fig. 2a SMF modification with CoO_x and MnO_x showed slightly better conversion than unmodified SMF, whereas, at 1000 ppm, all the electrodes showed nearly same activity. Hence, the absence of the catalytic effect at 1000 ppm of IP may be due to quick deactivation of the catalyst. For 500 of IP the activity of the studied catalysts followed the trend $\text{MnO}_x/\text{SMF} > \text{CoO}_x/\text{SMF} > \text{SMF}$.

As seen earlier that with decreasing VOC concentration, selectivity to CO_2 increases. In order to confirm this observation VOC concentration was further decreased to 250 ppm. Fig. 3a and b presents the influence of the applied voltage on the conversion of 250 ppm of IP. As seen from Fig. 3a, SMF catalyst showed poor activity throughout the range of SIE. At 160 J/l SMF shows ~60% conversion that increased to 100% at 295 J/l, whereas, with CoO_x and MnO_x/SMF electrodes, 100% conversion of IP was observed even at 235 J/l. This better activity of modified electrodes may be due to the formation of strong oxidant atomic oxygen.

Selectivity to the CO_x has been shown in Fig. 3b. As seen from Fig. 3b, for 250 ppm of IP ~100% selectivity to CO_x was observed at 235 J/l, whereas under the same conditions, for 500 and 1000 ppm of IP, selectivity to CO_2 was only around 90%. Hence, during the destruction of 250 ppm of IP, SIE of 235 J/l is required in order to avoid carbon deposit. CoO_x and MnO_x/SMF showed better CO_x selectivity than unmodified SMF, which is in agreement with the earlier observations. It is worth mentioning that at 235 J/l, CoO_x and MnO_x/SMF showed 100% conversion. Interestingly, with increasing SIE, the CO_2 selectivity increases over the catalytic electrodes under the study. SMF showed ~40% selectivity to CO_2 at 295 J/l, whereas MnO_x/SMF showed around 45% CO_2 selectivity even at 160 J/l and reached 80% at 295 J/l. A similar trend was observed on other CoO_x/SMF electrode. Hence, selectivity towards total oxidation of IP increases with metal oxide modified electrodes. The

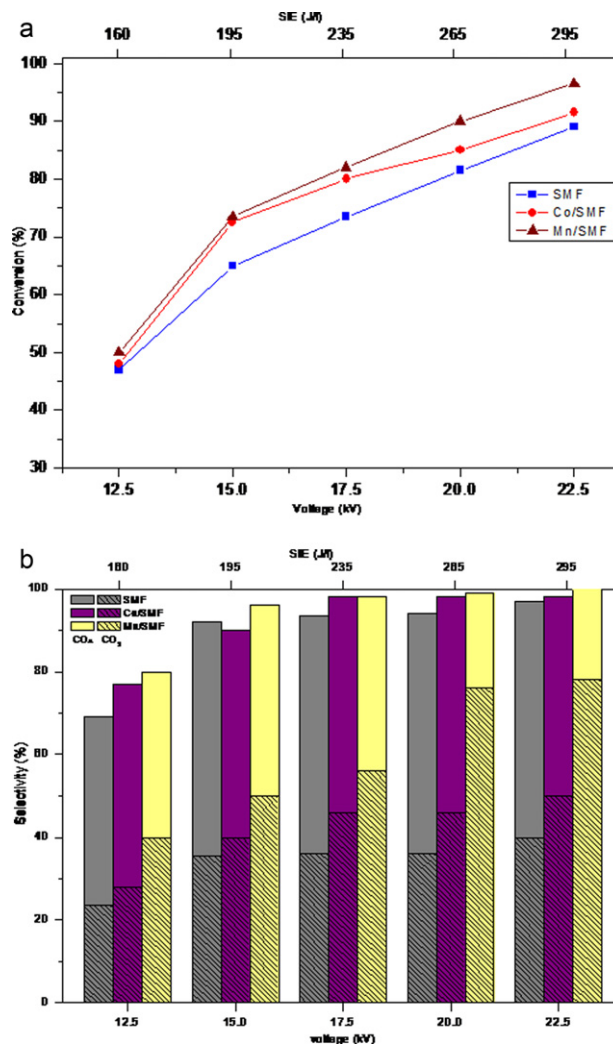


Fig. 2. (a) Influence of SMF modification and SIE on the conversion of IP (SIE 160–295 J/l and 500 ppm of IP). (b) Influence of SMF modification and SIE on selectivity to CO_x and CO_2 (SIE 160–295 J/l and 500 ppm of IP).

MnO_x/SMF showed better performance towards total oxidation compared to CoO_x/SMF .

As seen from the earlier studies, NTP reactor shows better performance with decreasing VOC concentration. In order to ensure this observation, IP concentration was further decreased to 100 ppm. As seen from Fig. 4, SMF electrode, conversion increases with increasing applied voltage and reaches ~100% only at 295 J/l, whereas, CoO_x and MnO_x/SMF showed better activity over SMF throughout the SIE range of the present study. Both these catalytic electrodes showed close to 100% conversion at SIE higher than 195 J/l. It is worth mentioning that 195 J/l is nearly equal to heating a liter of gas to ~200 °C.

Fig. 4b represents the selectivity to CO_x during destruction of 100 ppm of IP. Selectivity to CO_x increases with increasing voltage and reached 100% (no carbon deposit) on CoO_x and MnO_x ~195 J/l, whereas it was higher than 235 J/l over SMF. Fig. 4b also presents CO_2 selectivity over various catalysts during destruction of 100 ppm of IP. As seen from Fig. 4b, SMF showed only ~50% selectivity to CO_2 at 295 J/l, whereas 90% selectivity to CO_2 was observed over MnO_x/SMF at 195 J/l (15 kV). It is worth mentioning that with MnO_x/SMF catalyst, at 195 J/l, the conversion was ~100% (Fig. 4a) and there was no polymeric carbon deposit (Fig. 4b). Hence, the DBD reactor with catalytic SMF electrode showed remarkable activity during the destruction of IP.

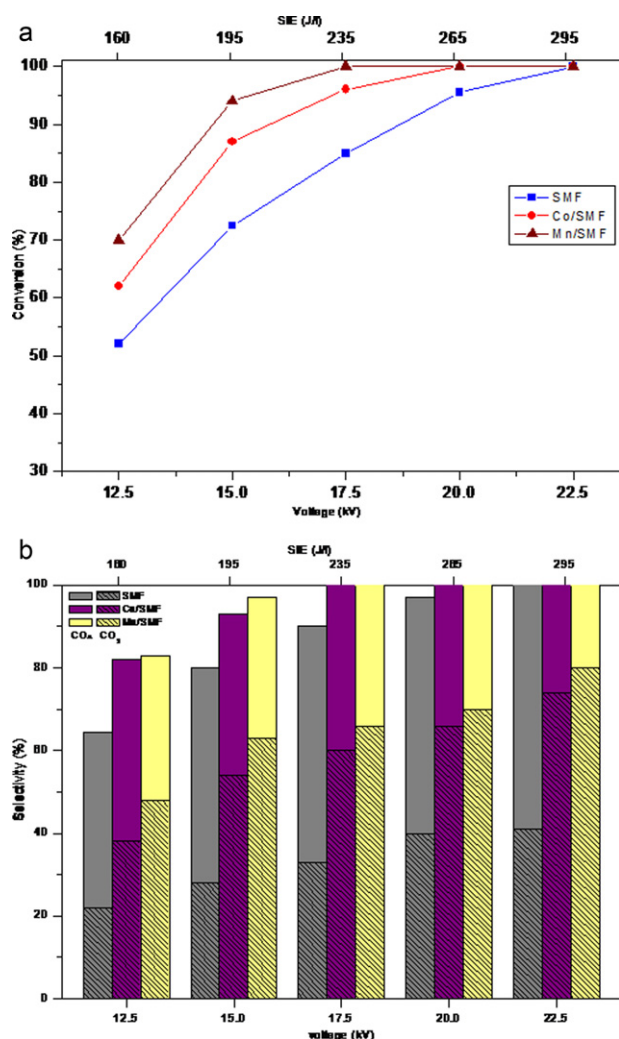


Fig. 3. (a) Influence of SMF modification and SIE on the conversion of IP (SIE 160–295 J/l and 250 ppm of IP). (b) Influence of SMF modification and SIE on selectivity to CO_x and CO₂ (SIE 160–295 J/l and 250 ppm of IP).

3.2. Influence of applied voltage and frequency on the performance of MnO_x/SMF catalytic electrode during the destruction of 100 ppm of isopropanol

From the above studies it is clear that SMF modification by metal oxides mainly resulted in higher performance of the DBD reactor and among Co and Mn oxides, MnO_x modification showed best performance over other electrodes during the destruction of IP in the SIE range 160–295 J/l, which was applied by varying the voltage between 12.5 and 22.5 kV at a fixed frequency of 200 Hz. However, SIE can also be varied by changing both voltage and frequency. Further studies were aimed at achieving the total oxidation of 100 ppm of IP over MnO_x catalytic electrode in the SIE range 160–725 J/l by changing the applied voltage between 12.5 and 22.5 kV and frequency in the range 200–275 Hz. Fig. 5a presents the conversion of 100 ppm of IP as a function of SIE over MnO_x/SMF electrode. As seen from Fig. 5a, at 200 Hz, ~100% conversion was achieved at a SIE > 195 J/l (15 kV) and increasing frequency to 250 Hz and 275 Hz has not shown any significant change in the conversion as ~100% conversion was obtained at SIE ≥ 200 J/l.

Fig. 5b also presents the selectivity profile of the CO and CO₂ during the destruction of 100 ppm of IP as a function of SIE. As no other hydrocarbon except IP was observed at the outlet, the selectivity to solid deposits can be estimated as (100 – S_{CO_x})%. As

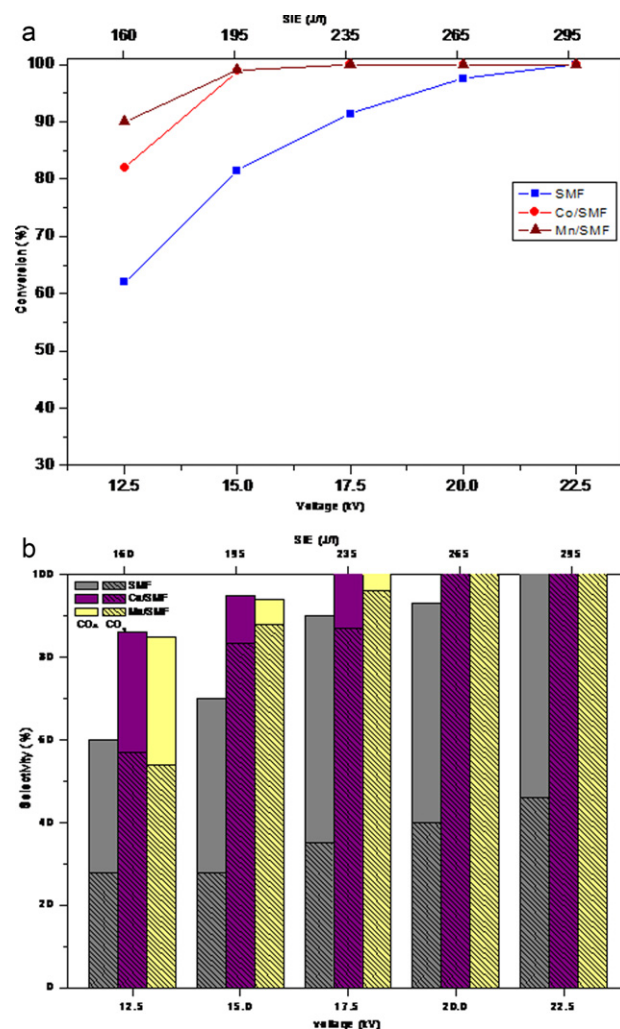


Fig. 4. (a) Influence of SMF modification and SIE on the conversion of IP (SIE 160–295 J/l and 100 ppm of IP). (b) Influence of SMF modification and SIE on selectivity to CO_x and CO₂ (SIE 160–295 J/l and 100 ppm of IP).

seen from Fig. 5b, increasing both voltage and frequency leads to a higher selectivity to CO_x, but also increases SIE. At any frequency, nearly 100% selectivity to CO_x (without solid deposit) was achieved at voltage higher 15.0 kV. Fig. 4b also represents the selectivity to CO₂, which also increases with increasing SIE. When SIE was varied in the range 160–295 J/l, a maximum of 100% selectivity to CO₂ was achieved at 195 J/l (200 Hz, 15 kV). With increasing frequency to 250 Hz, nearly the same selectivity was observed. Hence, with the novel DBD reactor presented in this work, it is possible to oxidize completely 100 ppm of IP at SIE ≥ 200 J/l.

3.3. Discussion

As seen from the above presented results, combination of catalyst with plasma showed improved performance. In general, the efficiency of NTP technique can be envisaged based on either reducing power consumption, and/or suppressing the undesired by-product formation. Among the alternatives to improve the efficiency of the plasma catalytic approach, increasing the residence time of VOCs in the plasma zone without changing the reactor size appears to be a promising approach. A combination of heterogeneous catalyst and non-thermal plasma seems to be the best choice, where increasing residence time of the adsorbate molecules in the plasma zone improves selectivity towards total oxidation. In practice, a catalyst may be combined with NTP in two ways: by

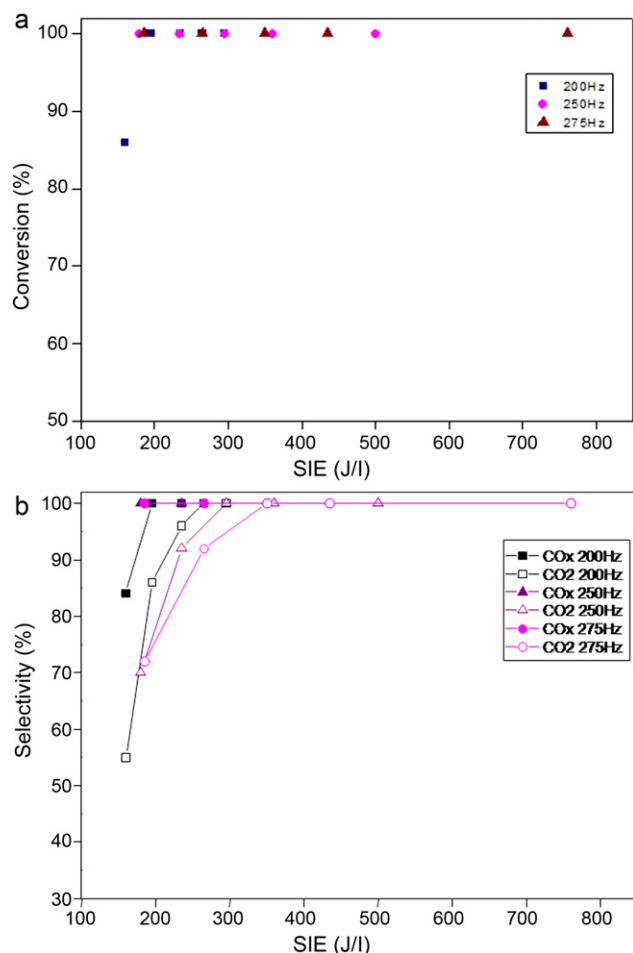


Fig. 5. (a) Influence of SIE on the conversion of IP (SIE 160–725 J/l and 100 ppm of IP). (b) Influence of SIE on the selectivity to CO_x and CO₂ (SIE 160–725 J/l and 100 ppm of IP).

introducing the catalyst in the discharge zone (In-plasma catalytic reactor, IPCR) or by placing the catalyst after the discharge zone (Post-plasma catalytic reactor, PPCR). The better performance of the plasma catalytic technique has been reported with the catalyst placed downstream to the discharge zone, mainly due to the oxidizing properties of long lived species like ozone. However, a synergy between NTP and catalysts is expected when the catalyst is placed in the discharge zone. Most of the chemically active species generated in the plasma are short-lived and cannot reach the catalyst surface in downstream configuration.

It is known that non-thermal plasma produces ozone from air by the ionization of oxygen molecules. Even though there is no direct correlation between the amount of ozone formed in the NTP reactor to its efficiency, nevertheless, the oxidation of various hydrocarbons in catalytic plasma reactor may be due to the decomposition of ozone on the catalyst surface leading to the formation of strong oxidizing species, mainly atomic oxygen [28–30]. During the present study, in the presence of 100 ppm of IP, ~900 ppm of ozone was observed, which decreases to 500 and 350 ppm with CoO_x and MnO_x/SMF, respectively. MnO_x/SMF catalytic electrode showed better performance during the destruction of IP compared to CoO_x/SMF and SMF. This observation can be explained based on the ozone decomposition efficiency as reported elsewhere [29]. MnO_x/SMF seems to be the active electrode in ozone decomposition. This suggests the formation of reactive oxygen species on MnO_x/SMF catalytic electrode at low energy consumption, which may be responsible for the higher performance

observed. The solid polymeric deposit may contain oxygenated functional groups as observed in the case of toluene oxidation [27].

4. Conclusions

Catalytic abatement of isopropanol (IP) in air was carried out in a DBD reactor with a catalytic SMF electrodes. Surface modification of SMF electrode with oxides of Co and Mn improved the total oxidation of IP forming only CO₂ and H₂O. The complete destruction of 100 ppm of IPA to CO_x and H₂O was achieved with a specific input energy (SIE) as low as ~200 J/l. Among the catalyst studied, 3 wt% MnO_x/SMF showed the best performance, where complete oxidation was achieved at SIE ~200 J/l. It has been proposed that *in situ* decomposition of ozone on MnO_x/SMF leads to the formation of reactive oxygen species, which are responsible for the observed higher activity of the MnO_x/SMF catalytic electrode.

Acknowledgement

Authors would like to thank DST- India for financial assistance. Authors would also like to thank Prof. Albert Renken and Prof. Kiwi-Minsker, EPFL Switzerland for their help.

References

- [1] <http://www.cdc.gov/niosh/npg/npgd0359.html>, NIOSH Pocket guide to chemical Hazards, 151 2005.
- [2] Pollution Prevention and Abatement Handbook, World Bank Group, 1998, 302.
- [3] AWMA, Air and Waste Management Association, Air Pollution Engineering Manual, Van Nostrand Reinhold, New York, 1992.
- [4] J.J. Coogan, Technologie Transfer # 97023244A-ENG, LANL, Feb. 1997.
- [5] John Zink Company, Innovations of Catalytic Combustion, International Symposium on Environmental Control of Combustion Processes, Honolulu, 1991.
- [6] S. Futamura, H. Einaga, H. Kabashima, L.Y. Hwan, Synergistic effect of silent discharge plasma and catalysts on benzene decomposition, *Catalysis Today* 89 (2004) 89.
- [7] U. Roland, F. Holzer, F.D. Kopinke, Improved oxidation of air pollutants in a non-thermal plasma, *Catalysis Today* 73 (2002) 315.
- [8] H.H. Kim, S.M. Oh, A. Ogata, S. Futamura, S. Futamura, A. Zhang, G. Prieto, T. Yamamoto, Factors and Intermediates governing byproduct distribution for decomposition of butane in non thermal plasma, *Transactions on Industry Applications* 34 (1998) 967.
- [9] H.H. Kim, S.M. Oh, A. Ogata, S. Futamura, Decomposition of gas phase benzene using plasma driven catalysts (PDC) reactor packed with Ag-TiO₂ catalysts, *Applied Catalysis B: Environmental* 56 (2005) 213.
- [10] C. Ayrault, J. Barrault, N. Blin-Simiand, F. Jorand, S. Pasquiers, A. Rousseau, J.M. Tatibouet, Oxidation of 2-heptanone in air by a DBD-type plasma generated within a honeycomb monolith supported Pt-based catalyst, *Catalysis Today* 89 (2004) 75.
- [11] B. Eliasson, U. Kogelschatz, Non equilibrium volume plasma chemical processing, *IEEE Transactions on Industry Applications* 19 (1991) 1063.
- [12] K. Yhang, B. Eliasson, U. Kogelschatz, Direct conversion of greenhouse gases to synthesis gas and C4 hydrocarbons over Zeolite HY promoted by a dielectric barrier discharge, *Industrial & Engineering Chemistry Research* 41 (2002) 1462.
- [13] U. Kogelschatz, Dielectric-barrier discharges: their history, discharge physics, and industrial applications, *Plasma Chemistry and Plasma Processing* 23 (1) (2003).
- [14] F. Holzer, U. Roland, U. Kopinke, Combination of non-thermal plasma and heterogeneous catalysis for oxidation of volatile organic compounds. Part 1. Accessibility of the intra-particle volume, *Applied Catalysis B: Environmental* 38 (2002) 163.
- [15] U. Roland, F. Holzer, F.D. Kopinke, Combination of non-thermal plasma and heterogeneous catalysis for oxidation of volatile organic compounds. Part 2. Ozone decomposition and deactivation of g-Al₂O₃, *Applied Catalysis B: Environmental* 58 (2005) 217.
- [16] U. Roland, F. Holzer, F.D. Kopinke, Combination of non-thermal plasma and heterogeneous catalysis for oxidation of volatile organic compounds. Part 3. Electron paramagnetic resonance (EPR) studies of plasma-treated porous alumina, *Applied Catalysis B: Environmental* 58 (2005) 227.
- [17] J.M. Gallardo-Amores, T. Armadori, G. Ramis, E. Finocchio, G. Busca, A study of anatase-supported Mn oxide as catalysts for 2-propanol oxidation, *Applied Catalysis B: Environmental* 22 (1999) 249.

- [18] Z. Falkenstein, Processing of C_3H_7OH , C_2HCl_3 and CCl_4 in flue gases using silent discharge plasmas (SDPs) enhanced by (V) UV at 172 nm and 253.7 nm, *Journal of Advanced Oxidation Technologies* 2 (1997) 223.
- [19] T. Oda, R. Yamashita, T. Takahashi, S. Masuda, Decomposition of gaseous organic contaminants by surface discharge induced plasma chemical processing—SPCP, *IEEE Transactions on Industry Applications* 32 (1996) 118.
- [20] D.E. Tevault, Carbon monoxide production in silent discharge plasmas of air and air–methane mixtures, *Plasma Chemistry and Plasma Processing* 7 (1987) 231.
- [21] B. Penetratnte, M.C. Hsiao, J.N. Bardsley, B.T. Merrit, G.E. Vogtlin, A. Kuthi, C.P. Burkhart, J.R. Bayless, Identification of mechanisms for decomposition of air pollutants by non-thermal plasma processing, *Plasma Chemistry and Plasma Processing* 6 (1997) 251.
- [22] T. Yamamoto, I.K. Mizuno, I. Tamori, A. Ogata, M. Nifuku, M. Michalska, G. Prieto, Catalysis-assisted plasma technology for carbon tetrachloride destruction, *IEEE Transactions on Industry Applications* 32 (1996) 100.
- [23] S. Futamura, A. Zhang, T. Yamamoto, The dependence of nonthermal plasma behavior of VOCs on their chemical structures, *Journal of Electrostatics* 42 (1997) 51.
- [24] V. Demidiouk, S.I. Moon, J.O. Chae, Toluene and butyl acetate removal from air by plasma-catalytic system, *Catalysis Communications* 4 (2003) 51.
- [25] A. Ogata, K. Mizuno, S. Kushiya, T. Yamamoto, Oxidation of dilute benzene in an alumina hybrid plasma reactor at atmospheric pressure, *Plasma Chemistry and Plasma Processing* 19 (1999) 383.
- [26] Ch. Subrahmanyam, M. Magureanu, L. Kiwi-Minsker, A. Renken, Catalytic abatement of volatile organic compounds assisted by non-thermal plasma. Part 1. A novel dielectric barrier discharge reactor containing catalytic electrode, *Applied Catalysis B: Environmental* 65 (2006) 150.
- [27] Ch. Subrahmanyam, L. Kiwi-Minsker, A. Renken, Plasma novel catalytic dielectric barrier discharge reactor for gas-phase abatement of isopropanol, *Plasma Chemistry And Plasma Processing* 27 (2007) 13.
- [28] B. Dhandapani, S.T. Oyama, Gas phase ozone decomposition catalysts, *Applied Catalysis B: Environmental* 11 (1997) 129.
- [29] W. Li, G.V. Gibbs, S.T. Oyama, Mechanism of ozone decomposition on a manganese oxide catalyst. 1. In situ Raman spectroscopy and ab initio molecular orbital calculations, *Journal* 120 (1998) 9041.
- [30] Hsin Liang Chen, How Ming Lee, Shiaw Huei Chen, Moo Been Chang, Sheng Jen Yu, Shou Nan Li, Removal of volatile organic compounds by single-stage and two-stage plasma catalysis systems: a review of the performance enhancement mechanisms, current status, and suitable applications, *Environmental Science & Technology* 43 (2009) 2216–2227.